

Effect of radiolysis of TODGA on the extraction of TODGA/n-dodecane toward Eu(III): An experimental and DFT study (Postprint)

Authors: Zhang, Hang, Ao, Yin-Yong, Wang, Yue, Zhao, Shang-Jie, Sun, Jia-Yang, Zhai, Mao-Lin, Li, Jiu-Qiang, Peng, Jing, Li, Hui-Bo, Peng, Jing, Li, Hui-Bo

Date: 2023-06-06T00:00:00+00:00

Abstract

N,N,N',N'-tetraoctyldiglycolamide (TODGA) is one of the most promising extractants for treating high-level liquid waste in nuclear fuel reprocessing. This study investigated the gamma radiolysis of TODGA (0.2 mol/L) in n-dodecane (nDD) solution, both with and without pre-equilibration with 3.0 mol/L HNO₃, using high-performance liquid chromatography (HPLC) and ultra-performance liquid chromatography-quadrupole time-of-flight mass spectrometry (UPLC-QTOF-MS), and compared it with the gamma radiolysis of pure TODGA. The concentration of TODGA in the studied systems decreased exponentially with increasing absorbed dose. Additionally, pre-equilibration with 3.0 mol/L HNO₃ had a slight effect on the gamma radiolysis of TODGA in nDD. In the investigated extraction systems, seven radiolysis products resulting from the cleavage of C–C, C–O, and C–N bonds in TODGA were identified. The effect of gamma radiation on the extraction of Eu(III) by TODGA/nDD was evaluated for the first time using a combined approach of extraction experiments and density functional theory (DFT) calculations, systematically comparing the complexation of Eu(III) with TODGA and its radiolysis products. Based on the radiolysis kinetic model of TODGA, the slope curve of Eu(III) distribution ratio (DEu) versus absorbed dose, and fluorescence titration analysis, an empirical equation relating absorbed dose to DEu was successfully obtained. Below 300 kGy, the experimental DEu values for TODGA/nDD showed good agreement with the obtained empirical equation. Conversely, at high absorbed doses, the experimental DEu values were higher than the theoretical DEu values based on the empirical equation, because TODGA radiolysis products with similar coordination structures still possess partial complexation ability toward Eu(III), which was confirmed by DFT calculations. This work provides a method for predicting the extraction

distribution ratios of irradiated extractant systems and understanding complex extraction processes.

Full Text

Effect of TODGA Radiolysis on the Extraction of Eu(III) by TODGA/n-Dodecane: An Experimental and DFT Study

Hang Zhang^{1,2‡}, Yin-Yong Ao^{3‡}, Yue Wang², Shang-Jie Zhao¹, Jia-Yang Sun^{1,2}, Mao-Lin Zhai², Jiu-Qiang Li², Jing Peng^{2*}, Hui-Bo Li^{1*}

¹ Department of Radiochemistry, China Institute of Atomic Energy, Beijing 102413, China

² Beijing National Laboratory for Molecular Sciences, Radiochemistry and Radiation Chemistry Key Laboratory for Fundamental Science, College of Chemistry and Molecular Engineering, Peking University, Beijing 100871, China

³ Institute of Nuclear Physics and Chemistry, China Academy of Engineering Physics, Mianyang 621900, China

‡ These authors contributed equally to this work.

Corresponding Authors: jpeng@pku.edu.cn, hb0012@sina.com

Abstract

N,N,N',N'-Tetraoctyl diglycolamide (TODGA) is one of the most promising extractants tailored for high-level liquid radioactive waste treatment during nuclear fuel reprocessing. In this study, the γ -radiolysis of TODGA (0.2 mol/L) in n-dodecane (nDD) solution, both with and without pre-equilibrated 3.0 mol/L HNO₃, was investigated using HPLC and UPLC-QTOF-MS and compared with the γ -radiolysis of neat TODGA. With increasing absorbed doses, the concentration of TODGA decreased exponentially for all studied systems. Moreover, pre-equilibration with HNO₃ (3.0 mol/L) only slightly influenced the γ -radiolysis of TODGA in nDD. Seven radiolytic products generated from the rupture of C–C, C–O, and C–N bonds in TODGA were identified in the extraction system. The influence of γ -radiation on the TODGA/nDD system for Eu(III) extraction was evaluated using a novel combination of extraction experiments and density functional theory (DFT) calculations, in which the complexation of Eu(III) with TODGA and its radiolytic products was systematically compared. Based on the radiolysis kinetic model of TODGA, the slope curve of the distribution ratio of Eu(III) (D_{Eu}) versus absorbed dose, and fluorescence titration analysis, an empirical equation relating absorbed dose and D_{Eu} was successfully obtained. Below 300 kGy, the experimental D_{Eu} values agreed well with the empirical equation for TODGA/nDD. Conversely, at high absorbed doses, the experimental D_{Eu} was higher than the theoretical D_{Eu} predicted by

the empirical equation because radiolytic products with coordination structures similar to TODGA still possessed partial complexation ability toward Eu(III), as confirmed by DFT calculations. This work provides a method to predict the extraction distribution ratio of an irradiated extractant system and enhances understanding of the complex extraction process.

Keywords: TODGA; Radiolytic products; Extraction; Density functional theory; Complexation

1. Introduction

Spent nuclear fuel (SNF) reprocessing generates high-level liquid radioactive waste (HLLW) composed of unextracted U and Pu, long-lived fission products (^{129}I , ^{99}Tc , ^{135}Cs , and ^{93}Zr), short-lived fission products (^{90}Sr and ^{137}Cs), minor actinides (MAs) (Np, Am, and Cm), and stable lanthanide isotopes (Eu, Nd, La, Tb, Pr, Gd, Sm, Ce, and Pm) [1–10]. To reduce the radiotoxicity and volume of HLLW and improve resource utilization, partitioning and transmutation strategies have been explored to shorten the half-life of long-lived radioisotopes. However, the transmutation efficiency of MAs is limited by the high thermal neutron capture cross-sections of several lanthanide isotopes due to competition for available neutrons [11, 12]. Thus, separating MAs from lanthanides (Lns) before transmutation is crucial.

During the liquid–liquid extraction process, N,N,N',N'-tetraoctyl diglycolamide (TODGA) has proven efficient for extracting actinides (Ans) and lanthanides [2, 13–16]. TODGA is a tridentate ligand that shows high distribution ratios for Lns(III)/Ans(III) because the hydrophilic groups exhibit stable metal coordination in the aqueous phase while the hydrophobic groups ensure solubility in the organic phase [17, 18]. It has been employed in several processes, such as the innovative Selective ActiNide EXtraction (i-SANEX) process [19, 20] and the EUROpean Grouped Actinide EXtraction (EURO-GANEX) process [21, 22]. The i-SANEX process first utilizes an organic solution containing TODGA (0.2 mol/L) and 1-octanol (5% v/v) to co-extract trivalent Lns and Ans from simulated HLLW, while Pd and Zr are masked by cyclohexane diamine tetraacetic acid (CDTA). Second, the co-extracted Mo and Sr are stripped using a 3.0 mol/L HNO_3 aqueous solution with CDTA (0.05 mol/L) and oxalic acid (0.2 mol/L) as scrubbing solvents, followed by a back-extraction step using an aqueous solution containing 2,6-bis(5,6-di(sulfophenyl)-1,2,4-triazin-3-yl)pyridine ($\text{SO}_3\text{-Ph-BTP}$) (1.8×10^{-2} mol/L) in HNO_3 (0.35 mol/L) for selective stripping of Ans(III). The final step involves stripping Lns(III) using a citrate buffer solution. Wilden et al. [19] demonstrated the effectiveness of this process, showing that Cm(III) and Am(III) were efficiently stripped (>99.8%) within six stages in the Ans product fraction, with excellent purity (only 0.4% Ru, 0.3% Sr, and 0.1% Lns(III) contamination). Lns(III) stripping was also efficient (>99.5%) within only four stages using a citric acid solution at pH 3.

The EURO-GANEX process consists of two cycles. In the first cycle, hydrogenated tetrapropene (TPH) containing N,N-di(2-ethylhexyl)isobutyramide (DEHiBA) (1.0 mol/L) selectively extracts U(VI). In the second cycle, extraction of Cm(III), Am(III), Pu(IV), Np(VI), and Lns(III) from the first cycle raffinate is achieved using N,N'-dimethyl-N,N'-dioctyl-2-(2-hexyloxyethyl)malonamide (DMDOHEMA) (0.5 mol/L) and TODGA (0.2 mol/L) in kerosene diluent, with CDTA (0.055 mol/L) as a masking agent to prevent Zr(IV) and Pd(II) extraction. Sr and Fe are extracted using HNO₃ (0.5 mol/L) from the loaded solvent, and trans-uranium elements (TRU) are back-extracted using an aqueous solution containing aceto-hydroxamic acid (AHA) and SO₃-Ph-BTP, while Lns(III) remains in the organic solution. Malmbeck et al. [23] successfully demonstrated the EURO-GANEX process via hot testing, showing efficient co-extraction of Pu(IV), Np(VI), Am(III), and Lns(III) from the EURO-GANEX raffinate during the first cycle, with Mo and Zr also co-extracted while other fission products were successfully rejected. Within six strip stages, 99.91% Np, 99.85% Pu, 99.90% Am, and co-extracted Mo and Zr were well back-extracted, while 99.9% Lns(III) was retained in the organic solution within four strip stages using an aqueous solution containing AHA and SO₃-Ph-BTP.

Previous studies have shown that TODGA provides significantly higher distribution ratios in alkanes such as n-dodecane (nDD) than in other diluents such as secondary ketones, primary alcohols, and secondary alcohols [24, 25]. The TODGA/nDD system can be applied to separate MAs and Lns from other fission products, after which individual element extraction can be simplified with additional processing, culminating in MA/Ln separation [26–28].

Because the extraction system is exposed to the radioactive environment formed by radionuclides, its radiation stability is an important factor to examine before practical application [29]. In solvent extraction processes, the γ -radiolysis of TODGA is problematic due to highly radioactive HLLW. Since the loss of TODGA and formation of radiolytic products during γ -radiation can adversely affect extraction performance toward metal ions, it is essential to measure the γ -radiolysis yield and radiolytic products of TODGA and study their effects on metal ion extraction. Radiolysis of TODGA in nDD under different conditions has been investigated [30, 31]. The magnitude of α -radiolysis of TODGA is lower than that of γ -radiolysis, though they produce similar radiolytic products [32]. This is attributed to the higher linear energy transfer of α particles compared to γ particles and the decreased radical yield of nDD by recombination in α -radiolysis. Although γ -radiolysis and extraction of TODGA have been investigated, the effect of γ -radiolysis and radiolytic TODGA products on extraction in the TODGA/nDD system has rarely been reported. Furthermore, predicting the extraction performance of irradiated extractant systems using equations would be highly beneficial for controlling the partition process. To the best of our knowledge, the mathematical correlation between extractant radiolysis and distribution ratio has seldom been studied.

In this work, because α and γ rays produce similar TODGA radiolysis products

and γ -radiation is easier to implement in the laboratory, the radiolytic behavior and γ -radiation stability of TODGA in the 0.2 mol/L TODGA/nDD system and the 0.2 mol/L TODGA/nDD system pre-equilibrated with 3.0 mol/L HNO_3 were studied qualitatively and quantitatively and compared with neat TODGA radiolysis. The content and radiolysis products of TODGA were determined using HPLC and UPLC-QTOF-MS, respectively. Considering the chemical similarity between trivalent lanthanides and minor actinides and to avoid handling radioactive isotopes in standard laboratories, Eu(III) was selected as a model metal ion to assess the extraction performance of TODGA/nDD after γ -radiation. Density functional theory (DFT) calculations, which can estimate the coordination abilities of TODGA and its radiolytic products, were applied to explain the effect of radiolytic products on Eu(III) extraction. For the first time, a combination of theoretical calculations and extraction experiments demonstrated that radiolytic products maintain partial complexation, which capably explains the extraction behavior of irradiated samples. This study provides an in-depth understanding of the effects of γ -irradiation on the extraction behavior of the TODGA/nDD system.

2. Experimental

2.1 Materials

TODGA ($\text{C}_{20}\text{H}_{32}\text{N}_2\text{O}_8$) and ^1H NMR (Figures S1–S2). $\text{Eu}(\text{NO}_3)_3 \cdot 6\text{H}_2\text{O}$ (99.99%) was obtained from MREDA Technology Co., Ltd. Formic acid (LC-MS grade) was purchased from Thermo Fisher Scientific. Methanol (LC-MS grade) was purchased from Honeywell Trading (Shanghai) Co., Ltd. Aqueous dilutions were performed using ultrapure water (18.2 $\text{M}\Omega\cdot\text{cm}$). All other chemicals were of analytical grade and used without further purification.

2.2 Gamma Irradiation

TODGA and TODGA/nDD solutions, equilibrated with and without HNO_3 (3.0 mol/L) before γ -radiation, were irradiated in air at room temperature (25 ± 5 °C) using a ^{60}Co source (Department of Applied Chemistry, College of Chemistry, Peking University, China) with an absorbed dose rate of 6.6 kGy/h, as determined by a Fricke dosimeter.

2.3 Quantitative Analysis of TODGA After Irradiation

An HPLC method with UV detection (SPD-16, Shimadzu, Japan) was used for quantitative analysis of TODGA concentration in irradiated samples. Chromatographic separation was performed at 25 ± 5 °C using an Agilent HC-C18 column (5 μm , 4.6 mm \times 150 mm) with UV detection at 210 nm. The mobile phase consisted of ultrapure water with formic acid (1% v/v) (component A) and methanol (component B). The elution program was: 0–10 min, 30–100%

B; 10–20 min, 100% B; 20–22 min, 100–30% B. The flow rate was 1.0 mL/min with an injection volume of 20 μ L. Error values in quantitative analysis were within 5%.

2.4 Identification and Semi-Quantification of Radiolytic Products

Ultra-high pressure liquid chromatography (UPLC) (ACQUITY I-Class, Waters, USA) was performed using an Agilent HC-C18 column (5 μ m, 4.6 mm \times 150 mm) at 40 $^{\circ}$ C. The aqueous component was ultrapure water with formic acid (1% v/v) (A), and the organic component was methanol with formic acid (1% v/v) (B). The elution program was: 0–4 min, 30–100% B; 4–13 min, 100% B; 13–13.1 min, 100–30% B; 13.1–15 min, 30% B. The flow rate was 0.8 mL/min with a 1 μ L injection volume. Quadrupole time-of-flight mass spectrometry (QTOF-MS) (Vion IMS QToF, Waters, USA) conditions were: desolvation temperature 300 $^{\circ}$ C; source temperature 120 $^{\circ}$ C; desolvation gas flow 800 L/h; capillary voltage 2.8 kV; cone gas flow 50 L/h; positive mode. Data were acquired and processed using Waters UNIFI Scientific Information System with a mass target match tolerance of <5 ppm.

2.5 Extraction Experiments

TODGA was dissolved in nDD to obtain a 0.7 mL organic phase at 0.2 mol/L concentration. $\text{Eu}(\text{NO}_3)_3 \cdot 6\text{H}_2\text{O}$ was dissolved in 3.0 mol/L HNO_3 to obtain a 0.7 mL aqueous phase at 1000 mg/L concentration. Pre-equilibration of the organic extraction phase with 3.0 mol/L HNO_3 was performed before extraction. Extraction experiments were conducted at 298 ± 1 K using a vortex mixer at 2500 rpm (LPD2500, Leopard Scientific Instrument Co., Ltd, Beijing). Phase separation was achieved by centrifugation for 1 min at 5000 rpm (TGL-16M, Cence, Hunan). After dilution with ultrapure water, the aqueous phase was analyzed by ICP-MS (ELEMENT XR, Thermo Scientific, USA) to determine Eu(III) concentration.

The distribution ratio of Eu(III) (D_{Eu}) was calculated using Eq. (1). The phase ratio was 1:1 in extraction experiments.

$$D_{Eu} = \frac{C_i - C_f}{C_f} \quad (1)$$

where C_f and C_i represent the final and initial Eu(III) concentrations in the diluted aqueous phase, respectively. The extraction error rate was <5%.

2.6 Fluorescence Spectra Titration

Fluorescence emission spectra of titration experiments were recorded at 298 ± 1 K in a 1 cm path length cuvette using a fluorescence spectrophotometer (F7000, Hitachi, Japan). The TODGA concentration was 0.1 mol/L in acetonitrile, and the initial Eu(III) concentration was 0.001 mol/L in 2.0 mL acetonitrile.

TODGA solution was added in 4 μL increments, with mixing for 5 min after each addition (VORTEX 3, IKA, Germany). Titration experiments used an excitation wavelength of 395 nm; excitation and emission bandwidths were 2.5 nm. Spectra were recorded from 550–700 nm at 1 nm intervals. Single-component spectra of metal–ligand complexes and metal solvent species were obtained using the HyperSpec program.

2.7 Theoretical Calculations

DFT calculations incorporating electron correlation effects were performed at the B3LYP level using Gaussian 09 [33–35]. Relativistic effects of Eu atoms were investigated using quasi-relativistic effective core potentials (RECPs) and associated valence basis sets from the Stuttgart and Dresden groups [36–40]. Large-core RECPs containing 52 electrons were used in structural optimization of Eu(III) [39, 40]. All other C, N, O, and H atoms utilized the 6-31G(d) basis set. Geometrical optimization and electronic calculations were first performed at the B3LYP/6-31G(d)/RECP level under gas-phase conditions. Gibbs free energy (G_g), entropy (S_g), and enthalpy (H_g) were obtained under gas-phase conditions at 298.15 K using the same theory level.

To obtain Gibbs free energy (G_{aq}), entropy (S_{aq}), and enthalpy (H_{aq}) of species in the nDD phase at 298.15 K, all species were optimized at the B3LYP/6-31G(d)/RECP level in nDD to better predict solvation energy [41]. This approach employed the SMD universal continuum solvation model [42].

3. Results and Discussion

3.1 Quantitative Analysis of TODGA Under Different Conditions After γ -Ray Irradiation

TODGA/nDD, HNO_3 -TODGA/nDD, and neat TODGA were subjected to γ -irradiation at absorbed doses ranging from 20 to 500 kGy. Irradiated samples were analyzed quantitatively by HPLC-UV to assess radiolytic stability. Figure 1 [Figure 1: see original paper] shows that TODGA concentration decreased exponentially with increasing absorbed dose, suggesting pseudo-first-order degradation kinetics for all systems. Comparison of TODGA/nDD and HNO_3 -TODGA/nDD revealed that HNO_3 had little influence on TODGA radiolysis. Moreover, the radiolysis rate of TODGA in nDD solution was higher than that of neat TODGA. A dodecane-induced “sensitization effect” accelerates TODGA radiolysis due to efficient positive charge transfer by nDD solvents [43–46].

Because TODGA radiolysis follows pseudo-first-order kinetics, the radiolysis rate causes an exponential decrease in TODGA concentration. The radiolysis rate equation is defined by Equation (2):

$$\frac{dC_{TODGA}}{dR} = -C_{TODGA} \cdot k \quad (2)$$

The solution to the rate equation is presented as Equation (3):

$$\frac{C_{TODGA}}{C_{TODGA}^0} = e^{-kR} \quad (3)$$

where C_{TODGA} (mol/L) is the concentration of TODGA, C_{TODGA}^0 (mol/L) is the original concentration before γ -radiation, R (kGy) is the absorbed dose, and the dose constant k (kGy⁻¹) is the coefficient obtained by fitting the exponential curve.

The dose constant k can be used to scale the absorbed dose for exponential behavior [47]. Using all information acquired during irradiation experiments provides more accurate results, and standard statistical methods can assess result accuracy. Application of k to characterize exponential curves in terms of absorbed dose is analogous to traditional time-dependent kinetics. As expressed by Equation (3), the reciprocal absorbed dose follows first-order kinetics instead of reciprocal time.

Figure 1 shows C_{TODGA}/C_{TODGA}^0 of irradiated TODGA/nDD, HNO₃-TODGA/nDD, and neat TODGA as a function of absorbed dose (R).

If dose constants k for different systems can be obtained, Equation (4) can calculate the G value ($\mu\text{mol}/\text{J}$), known as the radiation chemical yield:

$$G = 10^3 \cdot C_{TODGA}^0 \cdot k \cdot \rho^{-1} \quad (4)$$

where ρ is the solution density (kg/L) ($\rho_{TODGA} = 0.91$ and $\rho_{0.2 \text{ mol/L TODGA/nDD}} = 0.77$ at 25 °C). Measurement results are shown in Table S1.

Table 1 presents the dose constants k and radiation chemical yields G for irradiated TODGA/nDD, HNO₃-TODGA/nDD, and neat TODGA. The dose constant k for TODGA in nDD is higher than that for neat TODGA due to the “sensitization effect,” while the radiation chemical yields G for TODGA/nDD and HNO₃-TODGA/nDD are lower than that for neat TODGA due to different initial concentrations of irradiated TODGA. These results agree with literature reports by Sugo et al. [43, 48] that the k value for 0.2 mol/L TODGA/nDD was 2.2×10^{-3} kGy⁻¹. Using the k value, we can predict that the absorbed doses for half-loss of TODGA concentration ($R_{0.5}$) in irradiated TODGA/nDD, HNO₃-TODGA/nDD, and neat TODGA will be approximately 330, 315, and 1060 kGy, respectively.

3.2 Identification and Semi-Quantitative Analysis of Radiolytic Products

Ultra-high-performance liquid chromatography with quadrupole time-of-flight mass spectrometry (UPLC-QTOF-MS) can identify and quantify complex mixtures of unknown compounds due to its high resolution and mass accuracy. The major radiolytic products of TODGA were identified by QTOF-MS and are presented in Table 2, with UPLC-QTOF-MS spectra shown in Figures S3–S9.

Seven mass signals were identified and attributed to possible radiolytic products of TODGA (P1–P7, Table 2). These products formed through rupture of C–N, C–O, and C–C bonds in TODGA. Four radiolysis routes after irradiation are shown in Scheme 1.

Figure 2 [Figure 2: see original paper] shows semi-quantitative analysis of radiolytic products P1–P7 in irradiated HNO_3 -TODGA/nDD and neat TODGA at absorbed doses from 20 to 500 kGy. Seven radiolytic products were found in both systems. Detector counts for products P1–P7 generally increased with absorbed dose. However, some products, such as P1 in irradiated neat TODGA, showed decreased detector counts from 400 to 500 kGy, likely because product formation from TODGA radiolysis was offset by self-radiolysis at higher doses. The rate of concentration increase was less than the rate of decrease for P1 in irradiated neat TODGA from 400–500 kGy.

Detector counts for all radiolytic products in irradiated TODGA/nDD were higher than in neat TODGA (Figure S10), indicating the “sensitization effect” of nDD, consistent with the radiolysis kinetics results. However, relative detector counts differed between the two systems. For example, P6 count was less than P4 in irradiated neat TODGA, but the converse was true for irradiated HNO_3 -TODGA/nDD. This can be attributed to different reaction mechanisms: irradiated neat TODGA produces radical cations by direct ionization, whereas in irradiated TODGA/nDD, nDD radical cations may transfer charge to TODGA molecules, leading to TODGA radiolysis [43, 49].

3.3 Influence of γ -Ray Irradiation on Eu(III) Extraction by the TODGA System

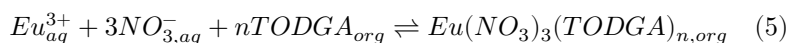
Neat TODGA and HNO_3 -TODGA/nDD were subjected to γ -ray irradiation at absorbed doses from 50 to 500 kGy. Irradiated neat TODGA was diluted with nDD to 0.2 mol/L. These organic phases were used to extract Eu(III) from 3.0 mol/L HNO_3 aqueous phase to evaluate extraction performance.

As shown in Figure 3 [Figure 3: see original paper], D_{Eu} decreased with increasing absorbed dose, but more slowly for irradiated TODGA than for irradiated HNO_3 -TODGA/nDD, indicating that γ -ray irradiation of the ligand significantly affected Eu(III) extraction. This further confirms that nDD presence increased TODGA radiolysis. However, the HNO_3 -TODGA/nDD system still maintained a high D_{Eu} (2.2×10^3) even at 500 kGy.

3.4 Slope Analysis and Fluorescence Titration

Before DFT calculations investigating complexation of TODGA and its radiolytic products with Eu(III), we assessed the stoichiometry of Eu ions and TODGA ligands in the extraction reaction via slope analysis of $\log D_M$ versus $\log[L]_{org}$.

The extraction reaction of Eu(III) by TODGA is expressed by Equation (5):



The extraction equilibrium concentration constant, K_{ex} , is described by Equation (6):

$$K_{ex} = \frac{[Eu(NO_3)_3(TODGA)_n]_{org}}{[Eu^{3+}]_{aq}[NO_3^-]_{aq}^3[TODGA]_{org}^n} \quad (6)$$

The distribution ratio, D_{Eu} , is defined by Equation (7):

$$D_{Eu} = \frac{[Eu(NO_3)_3(TODGA)_n]_{org}}{[Eu^{3+}]_{aq}} \quad (7)$$

Substituting Equation (7) into Equation (6) and transforming to logarithmic form yields Equation (8):

$$\log D_{Eu} = \log K_{ex} + n \log [TODGA]_{org} + 3 \log [NO_3^-]_{aq} \quad (8)$$

The n value, representing the average number of TODGA molecules coordinated to one metal ion, can be calculated from Equation (8). The plot in Figure 4 [Figure 4: see original paper] of $\log D_{Eu}$ versus $\log [TODGA]_{org}$ at constant 3.0 mol/L HNO_3 shows a slope of 3.10 ± 0.11 , indicating that Eu(III) forms complexes with three TODGA molecules.

Complexation studies were also performed using fluorescence titration of TODGA with Eu(III). Figure 5 [Figure 5: see original paper] displays normalized fluorescence emission spectra from transitions ${}^5D_0 \rightarrow {}^7F_1$ and ${}^5D_0 \rightarrow {}^7F_2$ at different Eu(III):TODGA ratios. The ${}^5D_0 \rightarrow {}^7F_1$ transition at 593 nm (magnetic-dipole) is independent of the ligand field, while the ${}^5D_0 \rightarrow {}^7F_2$ transition at 617 nm (electric-dipole) is hypersensitive to the ligand field, with intensity depending on coordination symmetry around the metal ion [50]. With TODGA addition, the ligand field change gradually transformed the single peak at 617 nm into a double peak, fully formed at M:L = 1:3, indicating gradual occupation of the Eu(III) inner coordination sphere by TODGA.

Single-component spectra obtained from fluorescence emission spectra (Figure 6 [Figure 6: see original paper]) revealed $[Eu(TODGA)_n]^{3+}$ complexes ($n = 1-3$)

and Eu(III) solvent species. No complexes with $n \geq 4$ were observed, confirming a Eu(III):TODGA ratio of 1:3.

While many studies show Ln(III):DGA structures form 1:3 complexes, the slope value has been debated. Antonio et al. [53] elucidated the inner coordination sphere of Eu(III)-TODGA using X-ray absorption spectroscopy (XAS), showing each TODGA molecule provides tridentate coordination through one ether O atom and two carbonyl O atoms to Eu(III), with a coordination number of nine. Turanov et al. [54] found a slope of 3.28 ± 0.04 for Eu(III) extraction by TODGA in n-decane containing 0.002 mol/L dinonylnaphtalene sulfonic acid (HDNNS). Pathak et al. [55] investigated solvent type, extraction acidity, and TODGA concentration effects on luminescence lifetime, finding $\text{Eu}(\text{TODGA})_3^{3+}$ species formation at various TODGA:Eu ratios. Sasaki et al. [56] reported that extracted Eu(III) complexes require three or four TODGA molecules and three nitrate ions for stability in non-polar diluents. Zhu et al. [57] found a slope of 3.9 for Eu(III), suggesting $\text{M}(\text{TODGA})_4(\text{NO}_3)_3$ species formation. However, this work determined a 1:3 complexation ratio for TODGA with Eu(III).

Theoretical D_{Eu} values at different TODGA concentrations can be obtained using Equation (8). Linear fitting (Figure 4) yields Equation (9):

$$\log D_{Eu} = 3.10 \log[\text{TODGA}]_{org} + 6.75 \quad (9)$$

Equation (10) from Figure 1 for irradiated HNO_3 -TODGA/nDD describes the exponential radiolysis relationship between TODGA concentration and absorbed dose:

$$\frac{C_{\text{TODGA}}}{C_{\text{TODGA}}^0} = e^{-2.20 \times 10^{-3} R} \quad (10)$$

Substituting Equation (10) into Equation (9) yields Equation (11), an empirical equation relating D_{Eu} and absorbed dose:

$$\log D_{Eu} = 3.10 \log(0.2 \cdot e^{-2.20 \times 10^{-3} R}) + 6.75 \quad (11)$$

This enables construction of a mathematical relationship between D_{Eu} and absorbed dose.

Theoretical D_{Eu} values for absorbed doses of 50–500 kGy were obtained using Equation (11). As shown in Figure 7 [Figure 7: see original paper], experimental D_{Eu} values were higher than theoretical values after irradiation, particularly above 300 kGy for the HNO_3 -TODGA/nDD system. Below 300 kGy, experimental D_{Eu} closely matches theoretical D_{Eu} , indicating that D_{Eu} decrease is mainly related to TODGA concentration loss with only slight influence from radiolytic products.

Because some radiolytic products (P1 and P2) retain coordination structures similar to TODGA, their complexation with Eu(III) was investigated using DFT calculations.

3.5 Theoretical Calculations of Complexation of TODGA and Radiolytic Products with Eu(III)

Based on slope and fluorescence titration analyses, the Eu(III):TODGA stoichiometry is 1:3. Kimberlin et al. [58] reported that several radiolytic products with the TODGA skeleton form heteroleptic complexes with TODGA at 1:3 stoichiometry, as observed in ESI-MS spectra. Time-resolved laser fluorescence results showed no change in fluorescence peak shape before and after irradiation (Figure S11), but fluorescence lifetime gradually decreased with increasing absorbed dose (Figure S12), indicating that γ radiation did not change the M:L ratio of 1:3 but caused slight partial changes in fluorescent species.

DFT calculations investigated coordination abilities of TODGA and its radiolytic products with TODGA skeletons (P1 and P2). Figure 8 [Figure 8: see original paper] shows optimized structures of complexes formed by Eu(III) with the ligands. Calculations were performed for $[\text{Eu}(\text{TODGA})_2(\text{P}_n)]^{3+}$ ($n = 1-2$) and $[\text{Eu}(\text{TODGA})_3]^{3+}$ complexes. It is realistic that one TODGA molecule in the initial complex could be replaced by a radiolytic product to form mixed Ln-radiolytic product-TODGA complexes during γ irradiation, as observed by Kimberlin et al. [58] in ESI-MS spectra. Additionally, optimized structures and coordination abilities of $[\text{Eu}(\text{P}_n)_3]^{3+}$ ($n = 1-2$) were investigated to represent a more extreme coordination environment of Eu(III) after γ irradiation.

Changes in Gibbs free energy, entropy, and enthalpy for complexes formed by ligands (TODGA, P1, and P2) with Eu(III) are shown in Table 3. $[\text{Eu}(\text{TODGA})_3]^{3+}$ formation has more negative ΔG in both gas phase (-2527.3 kJ/mol) and nDD phase (-1115.0 kJ/mol) than $[\text{Eu}(\text{TODGA})_2(\text{P}_n)]^{3+}$ and $[\text{Eu}(\text{P}_n)_3]^{3+}$ ($n = 1-2$) complexes. Coordination abilities of TODGA radiolytic products decreased, as reflected by changes in Eu-O bond length (Table 4). The average Eu-O bond length changed from 2.4911 \AA ($[\text{Eu}(\text{TODGA})_3]^{3+}$) to 2.5000 \AA ($[\text{Eu}(\text{P}2)_3]^{3+}$), indicating declining coordination ability. These results show TODGA has better coordination ability than its radiolytic products, with the order: TODGA > P1 > P2. However, $[\text{Eu}(\text{TODGA})_2(\text{P}_n)]^{3+}$ and $[\text{Eu}(\text{P}_n)_3]^{3+}$ complexes ($n = 1-2$) still had high negative ΔG values in both phases. Theoretical calculations indicate that radiolytic products such as P1 and P2 maintain good coordination ability with Eu atoms, proving they retain partial complexation for Eu(III).

Consequently, experimental D_{Eu} values were higher than theoretical D_{Eu} values based solely on TODGA loss, particularly at high absorbed doses where radiolytic products accumulate. If P1 and P2 contents are determined accurately, combining them with TODGA content would enable more precise prediction of D_{Eu} for irradiated TODGA/nDD systems. This will be addressed in future

work. In previous experiments, radiolytic products P1 and P2 were difficult to synthesize, and P1 was insufficiently stable. Therefore, DFT calculations were used to evaluate coordination abilities of these products, justifying the experimental observation that D_{Eu} exceeded theoretical values at high doses.

4. Conclusions

In summary, γ -radiolysis of TODGA/nDD and HNO_3 -TODGA/nDD was investigated and compared with neat TODGA radiolysis by analyzing TODGA loss and liquid radiolytic products. With increasing absorbed dose, TODGA concentration decreased exponentially, and the dose constant for TODGA in nDD was higher than for neat TODGA due to the nDD “sensitization effect.” However, pre-equilibration with HNO_3 only slightly affected TODGA radiolysis in nDD. Seven radiolytic products were identified and semi-quantified by UPLC-QTOF-MS, and four radiolysis routes were proposed. D_{Eu} values for irradiated systems decreased after irradiation, but HNO_3 -TODGA/nDD irradiated at 500 kGy maintained a high D_{Eu} of 2.2×10^3 . For irradiated HNO_3 -TODGA/nDD, an empirical equation relating D_{Eu} and absorbed dose was derived by combining TODGA radiolysis kinetics with the TODGA-Eu(III) complexation equation, fitting well with experimental results below 300 kGy. DFT calculations demonstrated that TODGA radiolytic products with similar coordination structures possessed good coordination abilities with Eu atoms, causing experimental D_{Eu} to exceed theoretical D_{Eu} based on ligand content at high absorbed doses.

Acknowledgments

UPLC-QTOF-MS and ICP-MS measurements were performed at the Analytical Instrumentation Center of Peking University. We acknowledge assistance from PKUAIC (Dr. Jiang Zhou, Dr. Li Zhang, and Dr. Jia-Hui Liu). The authors also thank Prof. Song-Dong Ding (Sichuan University) for providing TODGA.

References

1. S.A. Ansari, P.K. Mohapatra, A review on solid phase extraction of actinides and lanthanides with amide based extractants. *J. Chromatogr. A* 1499, 1–20 (2017). <https://doi.org/10.1016/j.chroma.2017.03.035>
2. S.A. Ansari, P. Pathak, P.K. Mohapatra et al., Chemistry of Diglycolamides: Promising Extractants for Actinide Partitioning. *Chem. Rev.* 112, 1751–1772 (2012). <https://doi.org/10.1021/cr200002f>
3. M. Salvatores, G. Palmiotti, Radioactive waste partitioning and transmutation within advanced fuel cycles: Achievements and

- challenges. *Prog. Part. Nucl. Phys.* 66, 144–166 (2011). <https://doi.org/10.1016/j.pnpnp.2010.10.001>
4. L. Rodríguez-Penalonga, B. Moratilla Soria, A Review of the Nuclear Fuel Cycle Strategies and the Spent Nuclear Fuel Management Technologies. *Energies* 10, 1235 (2017). <https://doi.org/10.3390/en10081235>
 5. X.L. Liu, G. Verma, Z.S. Chen et al., Metal-organic framework nanocrystal-derived hollow porous materials: Synthetic strategies and emerging applications. *The Innovation* 3, 100281 (2022). <https://doi.org/10.1016/j.xinn.2022.100281>
 6. Y.F. Zhang, H.X. Liu, F.X. Gao et al., Application of MOFs and COFs for photocatalysis in CO₂ reduction, H₂ generation, and environmental treatment. *EnergyChem* 4, 100078 (2022). <https://doi.org/10.1016/j.enchem.2022.100078>
 7. X. Wang, S.Q. Pan, Q.K. Zhao et al., The status of ITER radioactive waste management and enlightenment to CFETR radioactive waste management. *Nucl. Tech.* 45, 090603 (2022). <https://doi.org/10.11889/j.0253-3219.2022.hjs.45.090603> (in Chinese)
 8. L.Y. Zhen, J.J. Zhang, Y.H. Lin et al., Analysis of the accuracy of ¹⁴C in gaseous effluent of nuclear power plant by direct measurement method. *Nucl. Tech.* 45, 090301 (2022). <https://doi.org/10.11889/j.0253-3219.2022.hjs.45.090301> (in Chinese)
 9. G. Yang, J.R. Lin, X.Y. Yang et al., Adsorption properties of surrounding rock for ¹³⁷Cs in a cavern-type low and intermediate radioactive waste repository. *Nucl. Tech.* 45, 080301 (2022). <https://doi.org/10.11889/j.0253-3219.2022.hjs.45.080301> (in Chinese)
 10. S.Q. Meng, Y.S. Hu, T.M. Ruan, Impact of nickel and iron on PWR zirconium alloy surface CRUD formation and boron precipitation. *Nucl. Tech.* 45, 060602 (2022). <https://doi.org/10.11889/j.0253-3219.2022.hjs.45.060602> (in Chinese)
 11. M. Nilsson, K.L. Nash, Review Article: A Review of the Development and Operational Characteristics of the TALSPEAK Process. *Solvent Extr. Ion Exch.* 25, 665–701 (2007). <https://doi.org/10.1080/07366290701634636>
 12. W.H. Duan, T.X. Sun, J.C. Wang, An industrial-scale annular centrifugal extractor for the TRPO process. *Nucl. Sci. Tech.* 29, 46 (2018). <https://doi.org/10.1007/s41365-018-0395-z>
 13. Y. Sugo, Y. Sasaki, S. Tachimori, Studies on hydrolysis and radiolysis of N,N,N',N'-tetraoctyl-3-oxapentane-1,5-diamide. *Radiochim. Acta* 90, 161–165 (2002). https://doi.org/10.1524/ract.2002.90.3_2002.161
 14. D. Whittaker, A. Geist, G. Modolo et al., Applications of Diglycolamide Based Solvent Extraction Processes in Spent Nuclear Fuel Reprocess-

- ing, Part 1: TODGA. *Solvent Extr. Ion Exch.* 36, 223–256 (2018). <https://doi.org/10.1080/07366299.2018.1464269>
15. Z. Dong, W.J. Yuan, C. Liu et al., Th(IV) and U(VI) removal by TODGA in ionic liquids: extraction behavior and mechanism, and radiation effect. *Nucl. Sci. Tech.* 28, 62 (2017). <https://doi.org/10.1007/s41365-017-0214-y>
 16. A. Geist, U. Müllich, D. Magnusson et al., Actinide(III)/Lanthanide(III) Separation Via Selective Aqueous Complexation of Actinides(III) using a Hydrophilic 2,6-Bis(1,2,4-Triazin-3-Yl)-Pyridine in Nitric Acid. *Solvent Extr. Ion Exch.* 30, 433–444 (2012). <https://doi.org/10.1080/07366299.2012.671111>
 17. P.K. Nayak, R. Kumaresan, K.A. Venkatesan et al., Extraction Behavior of Am(III) and Eu(III) from Nitric Acid Medium in Tetraoctyldiglycolamide-Bis(2-Ethylhexyl)Phosphoric Acid Solution. *Sep. Sci. Technol.* 49, 1186–1191 (2014). <https://doi.org/10.1080/01496395.2013.874357>
 18. M.B. Singh, S.R. Patil, A.A. Lohi et al., Insight into nitric acid extraction and aggregation of N,N,N',N'-Tetraoctyl diglycolamide (TODGA) in organic solutions by molecular dynamics simulation. *Sep. Sci. Technol.* 53, 1361–1371 (2018). <https://doi.org/10.1080/01496395.2018.1445107>
 19. A. Wilden, G. Modolo, P. Kaufholz et al., Laboratory-Scale Counter-Current Centrifugal Contactor Demonstration of an Innovative-SANEX Process Using a Water Soluble BTP. *Solvent Extr. Ion Exch.* 33, 91–108 (2015). <https://doi.org/10.1080/07366299.2014.952532>
 20. G. Modolo, A. Wilden, P. Kaufholz et al., Development and demonstration of innovative partitioning processes (i-SANEX and 1-cycle SANEX) for actinide partitioning. *Prog. Nucl. Energ.* 72, 107–114 (2014). <https://doi.org/10.1016/j.pnucene.2013.07.021>
 21. J. Brown, F. McLachlan, M. Sarsfield et al., Plutonium Loading of Prospective Grouped Actinide Extraction (GANEX) Solvent Systems based on Diglycolamide Extractants. *Solvent Extr. Ion Exch.* 30, 127–141 (2012). <https://doi.org/10.1080/07366299.2011.609378>
 22. K. Bell, C. Carpentier, M. Carrott et al., Progress Towards the Development of a New GANEX Process. *Procedia Chemistry* 7, 392–397 (2012). <https://doi.org/10.1016/j.proche.2012.10.061>
 23. R. Malmbeck, D. Magnusson, S. Bourg et al., Homogenous recycling of transuranium elements from irradiated fast reactor fuel by the EURO-GANEX solvent extraction process. *Radiochim. Acta* 107, 917–929 (2019). <https://doi.org/10.1515/ract-2019-0001>
 24. I. Kajan, M. Florianová, C. Ekberg et al., Effect of diluent on the extraction of europium(III) and americium(III) with N,N,N',N'-tetraoctyl diglycolamide (TODGA). *RSC Adv.* 11, 36707–36718 (2021). <https://doi.org/10.1039/D1RA07534A>

25. S. Panja, P.K. Mohapatra, S.C. Tripathi et al., Role of organic diluents on Am(III) extraction and transport behaviour using N,N,N',N'-tetraoctyl-3-oxapentanediamide as the extractant. *J. Membr. Sci.* 403–404, 71–77 (2012). <https://doi.org/10.1016/j.memsci.2012.02.022>
26. J. Veliscek-Carolan, Separation of actinides from spent nuclear fuel: A review. *J. Hazard. Mater.* 318, 266–281 (2016). <https://doi.org/10.1016/j.jhazmat.2016.07.027>
27. Y. Wang, Y.Y. Ao, W.J. Yuan et al., Extraction performance of Eu³⁺ by using heterocyclic N-donor ligands with different structures in ionic liquids: an experimental and theoretical study. *New J. Chem.* 42, 7206–7212 (2018). <https://doi.org/10.1039/C8NJ00517F>
28. C. Marie, P. Kaufholz, V. Vanel et al., Development of a Selective Americium Separation Process Using H₄TPAEN as Water-Soluble Stripping Agent. *Solvent Extr. Ion Exch.* 37, 313–327 (2019). <https://doi.org/10.1080/07366299.2019.1643569>
29. Y. Wang, J. Peng, W. Huang et al., A new strategy for identifying the water-insoluble radiolytic products of BPC6/ionic liquids and accessing their influence on the Cs extraction. *Radiat. Phys. Chem.* 165, 108408 (2019). <https://doi.org/10.1016/j.radphyschem.2019.108408>
30. C.A. Zarzana, G.S. Groenewold, B.J. Mincher et al., A Comparison of the γ -Radiolysis of TODGA and T(EH)DGA Using UHPLC-ESI-MS Analysis. *Solvent Extr. Ion Exch.* 33, 431–447 (2015). <https://doi.org/10.1080/07366299.2015.1012885>
31. P. Zsabka, K. Van Hecke, A. Wilden et al., Gamma radiolysis of TODGA and CyMe₄BTPPhen in the ionic liquid tri-n-octylmethylammonium nitrate. *Solvent Extr. Ion Exch.* 38, 212–235 (2020). <https://doi.org/10.1080/07366299.2019.1710918>
32. Y. Sugo, M. Taguchi, Y. Sasaki et al., Radiolysis study of actinide complexing agent by irradiation with helium ion beam. *Radiat. Phys. Chem.* 78, 1140–1144 (2009). <https://doi.org/10.1016/j.radphyschem.2009.06.031>
33. W.T. Xu, Y.F. Zhou, D.C. Huang et al., Luminescent sensing profiles based on anion-responsive lanthanide(III) quinolinecarboxylate materials: solid-state structures, photophysical properties, and anionic species recognition. *J. Mater. Chem. C* 3, 2003–2015 (2015). <https://doi.org/10.1039/C4TC02369B>
34. C. Lee, W. Yang, R.G. Parr, Development of the Colle-Salvetti correlation-energy formula into a functional of the electron density. *Phys. Rev. B* 37, 785–789 (1988). <https://doi.org/10.1103/PhysRevB.37.785>
35. A.D. Becke, Density-functional thermochemistry. III. The role of exact exchange. *J. Chem. Phys.* 98, 5648–5652 (1993). <https://doi.org/10.1063/1.464913>
36. W. Küchle, M. Dolg, H. Stoll et al., Energy-adjusted pseudopotentials for the actinides. Parameter sets and test calculations for thorium

- and thorium monoxide. *J. Chem. Phys.* 100, 7535–7542 (1994). <https://doi.org/10.1063/1.466847>
37. X. Cao, M. Dolg, Segmented contraction scheme for small-core actinide pseudopotential basis sets. *J. Mol. Struct.* 673, 203–209 (2004). <https://doi.org/10.1016/j.theochem.2003.12.015>
 38. M. Dolg, H. Stoll, A. Savin et al., Energy-adjusted pseudopotentials for the rare earth elements. *Theoret. Chim. Acta* 75, 173–194 (1989). <https://doi.org/10.1007/BF00528565>
 39. M. Dolg, H. Stoll, H. Preuss, A combination of quasirelativistic pseudopotential and ligand field calculations for lanthanoid compounds. *Theoret. Chim. Acta* 85, 441–450 (1993). <https://doi.org/10.1007/BF01112983>
 40. M. Dolg, H. Stoll, H. Preuss, Energy-adjusted ab initio pseudopotentials for the rare earth elements. *J. Chem. Phys.* 90, 1730–1734 (1989). <https://doi.org/10.1063/1.456066>
 41. H. Struebing, Z. Ganase, P.G. Karamertzanis et al., Computer-aided molecular design of solvents for accelerated reaction kinetics. *Nature Chem.* 5, 952–957 (2013). <https://doi.org/10.1038/nchem.1755>
 42. A.V. Marenich, C.J. Cramer, D.G. Truhlar, Universal Solvation Model Based on Solute Electron Density and on a Continuum Model of the Solvent Defined by the Bulk Dielectric Constant and Atomic Surface Tensions. *J. Phys. Chem. B* 113, 6378–6396 (2009). <https://doi.org/10.1021/jp810292n>
 43. Y. Sugo, Y. Izumi, Y. Yoshida et al., Influence of diluent on radiolysis of amides in organic solution. *Radiat. Phys. Chem.* 76, 794–800 (2007). <https://doi.org/10.1016/j.radphyschem.2006.05.008>
 44. H. Galán, A. Núñez, A.G. Espartero et al., Radiolytic Stability of TODGA: Characterization of Degraded Samples under Different Experimental Conditions. *Procedia Chem.* 7, 195–201 (2012). <https://doi.org/10.1016/j.proche.2012.10.033>
 45. H. Galán, C.A. Zarzana, A. Wilden et al., Gamma-radiolytic stability of new methylated TODGA derivatives for minor actinide recycling. *Dalton Trans.* 44, 18049–18056 (2015). <https://doi.org/10.1039/C5DT02484F>
 46. W.J. Yuan, C.Z. Wang, Y.Y. Ao et al., γ -Radiation effect on Th⁴⁺ extraction behaviour of TODGA/[C₂mim][NTf₂]: identification and extractability study of radiolytic products. *RSC Adv.* 6, 7626–7632 (2016). <https://doi.org/10.1039/C5RA25364K>
 47. B.J. Mincher, R.D. Curry, Considerations for choice of a kinetic fig. of merit in process radiation chemistry for waste treatment. *Appl. Radiat. Isot.* 5 (2000). [https://doi.org/10.1016/S0969-8043\(99\)00161-X](https://doi.org/10.1016/S0969-8043(99)00161-X)

48. R. Malmbeck, N.L. Banik, Radiolytic behaviour of a TODGA based solvent under alpha irradiation. *J. Radioanal. Nucl. Chem.* 326, 1609–1615 (2020). <https://doi.org/10.1007/s10967-020-07444-7>
49. S.P. Mezyk, B.J. Mincher, S.B. Dhiman et al., The role of organic solvent radical cations in separations ligand degradation. *J. Radioanal. Nucl. Chem.* 307, 2445–2449 (2016). <https://doi.org/10.1007/s10967-015-4582-7>
50. B. Rajamouli, P. Sood, S. Giri et al., A Dual-Characteristic Bidentate Ligand for a Ternary Mononuclear Europium(III) Molecular Complex – Synthesis, Photophysical, Electrochemical, and Theoretical Study. *Eur. J. Inorg. Chem.* 2016, 3900–3911 (2016). <https://doi.org/10.1002/ejic.201600508>
51. A. Wilden, G. Modolo, S. Lange et al., Modified Diglycolamides for the An(III) + Ln(III) Co-separation: Evaluation by Solvent Extraction and Time-Resolved Laser Fluorescence Spectroscopy. *Solvent Extr. Ion Exch.* 32, 119–137 (2014). <https://doi.org/10.1080/07366299.2013.833791>
52. A. Sengupta, P.K. Mohapatra, M. Iqbal et al., Spectroscopic investigations of Eu^{3+} -complexes with ligands containing multiple diglycolamide pendant arms in a room temperature ionic liquid. *J. Lumin.* 154, 392–401 (2014). <https://doi.org/10.1016/j.jlumin.2014.05.001>
53. M.R. Antonio, D.R. McAlister, E.P. Horwitz, An europium(III) diglycolamide complex: insights into the coordination chemistry of lanthanides in solvent extraction. *Dalton Trans.* 44, 515–521 (2015). <https://doi.org/10.1039/C4DT01775G>
54. N. Turanov, V. Karandashev, Synergistic Extraction of U(VI), Th(IV), and Lanthanides(III) from Nitric Acid Solutions Using Mixtures of TODGA and Dinonylnaphthalene Sulfonic Acid. *Solvent Extr. Ion Exch.* 36, 257–271 (2018). <https://doi.org/10.1080/07366299.2018.1459157>
55. P.N. Pathak, S.A. Ansari, S.V. Godbole et al., Interaction of Eu^{3+} with N,N,N',N'-tetraoctyl diglycolamide: A time resolved luminescence spectroscopy study. *Spectroc. Acta Pt. A-Molec. Biomolec. Spectr.* 73, 348–352 (2009). <https://doi.org/10.1016/j.saa.2009.02.040>
56. Y. Sasaki, P. Rapold, M. Arisaka et al., An Additional Insight into the Correlation between the Distribution Ratios and the Aqueous Acidity of the TODGA System. *Solvent Extr. Ion Exch.* 25, 187–204 (2007). <https://doi.org/10.1080/07366290601169345>
57. Z.X. Zhu, Y. Sasaki, H. Suzuki et al., Cumulative study on solvent extraction of elements by N,N,N',N'-tetraoctyl-3-oxapentanediamide (TODGA) from nitric acid into n-dodecane. *Anal. Chim. Acta* 527, 163–168 (2004). <https://doi.org/10.1016/j.aca.2004.09.023>

58. A. Kimberlin, D. Guillaumont, S. Arpigny et al., An experimental and computational look at the radiolytic degradation of TODGA and the effect on metal complexation. *New J. Chem.* 45, 12479–12493 (2021). <https://doi.org/10.1039/D1NJ01143J>

Note: Figure translations are in progress. See original paper for figures.

Source: ChinaXiv — Machine translation. Verify with original.